

3D-conformal very-high energy electron therapy as candidate modality for FLASH-RT: A treatment planning study for glioblastoma and lung cancer

Till Tobias Böhlen¹  | Jean-François Germond¹ | Erik Traneus² |
 Veronique Vallet¹ | Laurent Desorgher¹ | Esat Mahmut Ozsahin³ |
 François Bochud¹ | Jean Bourhis³ | Raphaël Moeckli¹ 

¹Institute of Radiation Physics, Lausanne University Hospital and Lausanne University, Lausanne, Switzerland

²RaySearch Laboratories, Stockholm, Sweden

³Department of Radiation Oncology, Lausanne University Hospital and Lausanne University, Lausanne, Switzerland

Correspondence

Raphaël Moeckli, Institute of Radiation Physics, Lausanne University Hospital and Lausanne University, Lausanne, Switzerland.
 Email: raphael.moeckli@chuv.ch

Funding information

ISREC Foundation thanks to a Biltema donation; Fondation pour le soutien de la recherche et du développement de l'oncologie

Abstract

Background: Pre-clinical ultra-high dose rate (UHDR) electron irradiations on time scales of 100 ms have demonstrated a remarkable sparing of brain and lung tissues while retaining tumor efficacy when compared to conventional dose rate irradiations. While clinically-used gantries and intensity modulation techniques are too slow to match such time scales, novel very-high energy electron (VHEE, 50–250 MeV) radiotherapy (RT) devices using 3D-conformed broad VHEE beams are designed to deliver UHDR treatments that fulfill these timing requirements.

Purpose: To assess the dosimetric plan quality obtained using VHEE-based 3D-conformal RT (3D-CRT) for treatments of glioblastoma and lung cancer patients and compare the resulting treatment plans to those delivered by standard-of-care intensity modulated photon RT (IMRT) techniques.

Methods: Seven glioblastoma patients and seven lung cancer patients were planned with VHEE-based 3D-CRT using 3 to 16 coplanar beams with equidistant angular spacing and energies of 100 and 200 MeV using a forward planning approach. Dose distributions, dose-volume histograms, coverage ($V_{95\%}$) and homogeneity ($HI_{98\%}$) for the planning target volume (PTV), as well as near-maximum doses ($D_{2\%}$) and mean doses (D_{mean}) for organs-at-risk (OAR) were evaluated and compared to clinical IMRT plans.

Results: Mean differences of $V_{95\%}$ and $HI_{98\%}$ of all VHEE plans were within 2% or better of the IMRT reference plans. Glioblastoma plan dose metrics obtained with VHEE configurations of 200 MeV and 3–16 beams were either not significantly different or were significantly improved compared to the clinical IMRT reference plans. All OAR plan dose metrics evaluated for VHEE plans created using 5 beams of 100 MeV were either not significantly different or within 3% on average, except for D_{mean} for the body, D_{mean} for the brain, $D_{2\%}$ for the brain stem, and $D_{2\%}$ for the chiasm, which were significantly increased by 1, 2, 6, and 8 Gy, respectively (however below clinical constraints). Similarly, the dose metrics for lung cancer patients were also either not significantly different or were significantly improved compared to the reference plans for VHEE configurations with 200 MeV and 5 to 16 beams with the exception of $D_{2\%}$ and D_{mean} to the

This is an open access article under the terms of the [Creative Commons Attribution-NonCommercial-NoDerivs](https://creativecommons.org/licenses/by-nc-nd/4.0/) License, which permits use and distribution in any medium, provided the original work is properly cited, the use is non-commercial and no modifications or adaptations are made.

© 2023 The Authors. *Medical Physics* published by Wiley Periodicals LLC on behalf of American Association of Physicists in Medicine.

spinal canal (however below clinical constraints). For the lung cancer cases, the VHEE configurations using 100 MeV or only 3 beams resulted in significantly worse dose metrics for some OAR. Differences in dose metrics were, however, strongly patient-specific and similar for some patient cases.

Conclusions: VHEE-based 3D-CRT may deliver conformal treatments to simple, mostly convex target shapes in the brain and the thorax with a limited number of critical adjacent OAR using a limited number of beams (as low as 3 to 7). Using such treatment techniques, a dosimetric plan quality comparable to that of standard-of-care IMRT can be achieved. Hence, from a treatment planning perspective, 3D-conformal UHDR VHEE treatments delivered on time scales of 100 ms represent a promising candidate technique for the clinical transfer of the FLASH effect.

KEYWORDS

3D-conformal radiotherapy (3D-CRT), FLASH effect, treatment planning, very-high energy electrons (VHEE)

1 | INTRODUCTION

Recent studies have found that large doses (≥ 5 Gy) delivered at ultra-high dose rates (UHDR) with short overall delivery durations (on time scales of 100 ms) result in reduced normal tissue damage while retaining tumor toxicity compared to doses delivered at conventional dose rates (CONV) ($\lesssim 0.1$ Gy/s).^{1,2} This experimental observation is called the “FLASH effect” and is receiving significant attention in the field of radiation therapy (RT), especially because dose-modifying factors (DMF) up to 1.8 have been reported for normal tissues, whilst almost no differences have been observed for tumors.^{3–5} Hence, UHDR dose delivery in sub-seconds has the potential to improve the therapeutic ratio compared to CONV RT. Encouraging preclinical results led to the treatment of the first human patient in 2018 with FLASH-RT using a 5.6 MeV UHDR electron beam.^{6,7} Additional clinical trials using FLASH-RT are currently underway or were recently concluded.^{8–10}

The UHDR irradiations that have demonstrated a substantial normal tissue sparing used single beam portals that delivered the whole dose to the irradiated tissue mostly in time scales of 100 ms.⁵ The execution of RT treatments at such time scales for deep-seated targets (> 5 cm) that are dosimetrically as conformal as standard-of-care RT pose a substantial technical challenge. UHDR RT devices proposed for the delivery of FLASH-RT to deep-seated targets encompass multiple beam modalities and associated delivery techniques including MV photon beams,¹¹ transmission (“shoot-through”) protons,^{12–16} 3D patient-specific range modulated proton and ion beams,^{16–19} and very-high energy electron (VHEE, 50–250 MeV) beams.^{20–27} The design and optimization of such devices are further complicated by the fact that the mechanisms of action for the FLASH effect are still being debated^{2,28} and precise temporal dose delivery conditions to obtain and

optimize the FLASH effect are still being investigated.²⁹ Preclinical studies suggest that the whole treatment dose needs to be delivered in time scales of 100 ms to obtain an optimized FLASH effect.^{5,30} This poses a demanding technical requirement for the delivery of conformal dose distributions in depth. In particular, conventional C-arm gantries with typical rotational speeds of one rotation per minute are not suited for delivering multiple beams within such short durations. Furthermore, intensity modulation or beam scanning also needs to be accomplished swiftly with severe requirements on timing. Hence, a relatively simple treatment technique that may achieve conformal dose delivery on such time scales to optimize its FLASH potential is the use of a limited number of fixed beam lines (FBL) that deliver collimated broad VHEE beams quasi-simultaneously using 3D-conformal RT (3D-CRT).^{20,21,25–27} More particularly, there are several initiatives that aim at the clinical implementation of VHEE-based FLASH-RT by applying or exploring the use of multi-directional collimated broad VHEE beams to administer UHDR treatments.^{21,27,31} For this VHEE-based 3D-CRT delivery approach, the achievable dosimetric conformity is of concern and will depend on the patient cohort and individual target characteristics.

Multiple comparative VHEE treatment planning studies have unanimously concluded that VHEE RT may deliver conformal dose distributions that are superior to those from state-of-the-art intensity modulated photon RT (IMRT) techniques.^{22–24,29,32–34} For these studies, inversely optimized VHEE treatment plans were created assuming VHEE RT devices that deliver multiple (mostly seven or more) coplanar fields using small beamlets with full-width-at-half-maximum sizes of a few millimeters. However, a large amount of FBL and small scanned beamlets may not be compatible with the temporal dose-delivery requirements producing an optimized FLASH effect with a UHDR VHEE device and may result in a

disproportionate size, cost, and technical complexity of the device.

The objective of this study was to investigate the feasibility of delivering dosimetrically conformal UHDR VHEE 3D-CRT treatments for selected clinical indications using collimated broad VHEE beams with a limited number of 100 to 200 MeV FBL. If a given VHEE device configuration could be shown to provide conformal absorbed dose distributions that are comparable to those achieved by current standard-of-care treatment modalities (i.e., non-inferiority design), then any additional sparing of normal tissues due to the FLASH effect while retaining tumor efficacy would contribute to further improve clinical outcome. Therefore, in this study we only evaluated absorbed dose (hereafter only “dose”) distributions and did not model the FLASH effect quantitatively, since this would imply additional assumptions. We performed treatment planning using multiple VHEE device configurations for glioblastoma multiforme (GBM) and lung cancer patient cases. This was motivated by the need to improve outcomes for glioblastoma and locally advanced non-small-cell lung cancer treatments^{35,36} as well as by preclinical experiments that reported DMF of 1.4 and more when irradiating brain and lung tissues with UHDR.^{1,3,5,37} At the same time, glioblastoma and lung cancers often present with comparatively simple planning target volume (PTV) shapes. This reduces the potential for dosimetric advantages of using intensity-modulated compared to 3D-conformal treatment techniques.³⁸ We compared the resulting dose distributions with those delivered clinically at our hospital using the standard of care, that is, volumetric arc therapy (VMAT) and helical tomotherapy (HT), hereafter referred to as IMRT reference plans, and we also evaluated the impact of the used energy and number of FBL on plan quality.

2 | MATERIALS AND METHODS

2.1 | Patient selection and IMRT reference plans

We selected seven GBM patients and seven lung cancer patients from our clinical database to be planned for VHEE RT applying the following criteria.

- We required the PTV extensions along each axis to be smaller than 15 cm, since UHDR broad beam irradiations are more difficult to perform for large field sizes.
- We excluded cases with complex PTV geometries involving simultaneous integrated boosts (SIB), multiple disjoint targets, and targets with major concave parts, since for such cases, 3D-CRT techniques can be expected to perform worse compared to intensity modulated techniques, as initially mentioned. A large

fraction of GBM and lung cancer patients fulfil these conditions.

- For lung cases, we also required that the PTV be larger than 30 cm³ to exclude small targets with good clinical outcome using standard of care.

We used the clinically applied IMRT plans that were generated for delivery with an Elekta Synergy linac (Elekta, UK, 6 and 10 MV VMAT) or a Tomotherapy unit (Accuray, USA, 6 MV HT) as reference plans. Clinical dose was computed with a Collapsed Cone dose engine (RayStation dose engine v5.2 and v5.5). Clinical GBM and lung plans were mostly planned using a conventionally fractionated scheme (30 × 2 Gy) with the median dose to the PTV D_{median} normalized to 60 ± 0.5 Gy. Plans not following this treatment scheme were renormalized to 60 Gy to facilitate a comparison of doses. Patient case and reference plan characteristics are summarized in Table 1.

2.2 | VHEE beam modelling and treatment planning

The VHEE beam model and its validation is described in detail elsewhere.²⁵ In brief, electron beams of different sizes and energies were simulated using the clinical electron Monte Carlo (eMC) algorithm (ElectronMonteCarlo v3.5) from RayStation (RayStation 9 IonPG) extended to VHEE energies (100–250 MeV). This eMC version uses a dedicated Monte Carlo code for the transport in the treatment head (merely used for tracking in the context of this work) and the VMC++ Monte Carlo code^{39,40} for energy transport and energy scoring in patients. The VMC++ code uses physics models that are applicable to several hundreds of MeV and that were benchmarked against general-purpose Monte Carlo codes and against measured VHEE data.²⁵ For this treatment planning study, we used an ideal cutout collimation and a cutout-to-isocentre distance of 50 cm. Parallel beams with energies of 100 and 200 MeV were simulated. As VHEE RT device designs with more than ten FBL have been proposed and appear technically feasible²⁰ (even if less FBL may reduce technical complexity, size and cost), we investigated different coplanar FBL configurations with 3, 5, 7, and 16 beams with equidistant angular spacing and identical energies, as specified in Table 2. We allowed couch kicks up to $\pm 30^\circ$ for GBM VHEE treatment plans provided that they did not result in collisions. Sixteen beams were chosen as a maximum, because such a configuration was used as a reference by other VHEE studies²² and it was found that plan quality did not substantially improve by adding further beams.²⁴ Five and seven coplanar beams with equidistant angles are constellations that are commonly used for IMRT treatments. Three beams were chosen as the lower limit of potential clinical interest. VHEE

TABLE 1 Summary of characteristics of patient cases and reference plans.

Indication	Patient number	PTV size median (range) (cm ³)	Prescribed dose (Gy)	Reference plans
GBM	7	183.2 (163.4–323.7)	60	3 VMAT 4 HT
Lung cancer	7	138.3 (35.8–211.8)	60	6 VMAT 1 HT

Abbreviations: HT, helical tomotherapy; PTV, planning target volume, VMAT, volumetric arc therapy.

TABLE 2 List of evaluated very-high energy electron beam configurations. Fixed beam lines are arranged coplanar with equidistant angular spacing and the first beam incident at 0°. Labels are used in the following to refer to specific VHEE configurations.

Label	Energy	Number of FBL	Angular spacing
16 × 200 MeV	200 MeV	16	22.5°
7 × 200 MeV	200 MeV	7	51.4°
5 × 200 MeV	200 MeV	5	72°
3 × 200 MeV	200 MeV	3	120°
5 × 100 MeV	100 MeV	5	72°

Abbreviations: FBL, Fixed beam lines; VHEE, very-high energy electron.

beams with small divergences create “high dose tunnels” in patient anatomies.²⁵ Hence, an uneven number of such coplanar VHEE beams with equidistant angles is usually preferable over an even number, since the dosimetric benefit of opposed VHEE beams is typically limited.²⁵ Furthermore, we chose VHEE beam configurations with energies of 100 and 200 MeV, since other studies indicate that this is the VHEE energy range that is more clinically useful in terms of depth-dose profile and lateral penumbra.^{22–25,41}

Seventy VHEE treatment plans were generated with 3D-CRT forward treatment planning. We conducted a manual iterative optimization employing a two-step sequential scheme. Our first step was to perform an iterative optimization of cutout shapes to maximize PTV coverage, usually $V_{95\%} > 95\%$ – 98% , while maximizing dose fall-off outside the PTV. For this purpose, the couch angle and beam weights were chosen to avoid critical organs-at-risk (OAR) and to decrease the mean dose to the patient body (D_{mean}). Secondly, we spared critical OAR while maintaining $V_{95\%}$ to be within 2% of the one of the reference plan (or better), by optimizing cutout shapes and beam weights further. Optimization was stopped when further OAR sparing resulted in a notable decrease of $V_{95\%}$ beyond the one of the reference plan. Dose distributions were normalized to a median dose (D_{median}) of 60 Gy in the PTV.

2.3 | Plan evaluation

We evaluated multiple target and OAR dose metrics of the VHEE and the reference plans. For the PTV,

we evaluated $V_{95\%}$ and the homogeneity index $HI_{98\%} = D_{98\%}/D_{2\%}$. For OAR, we evaluated the near-maximum dose ($D_{2\%}$) and the mean dose (D_{mean}). For the lung, we evaluated additionally $V_{5\text{ Gy}}$ and $V_{20\text{ Gy}}$. Box-and-whisker plots were used to display dose metrics. Outliers were plotted explicitly if they lay outside the interquartile range times 1.5. Symmetric organs (e.g., lungs, eyes, lenses, optic nerves), were pooled for combined evaluation. We employed two-sided Wilcoxon signed-rank tests for statistical analysis to compare the VHEE dose metrics to those of the reference plans. Differences in dose metrics were considered to be statistically significant for p -values below 0.05. For each clinical indication, dose metrics averaged over all patient cases were computed for the reference plans and percentage differences from these averages were evaluated for the VHEE plans. For some patient cases, not all OAR were delineated, present or of relevance (e.g., pituitary glands and main bronchus) and, hence, corresponding statistics are lower. Extraction of dose metrics was performed using python-based scripting capabilities of RayStation. Data analysis and visualization was equally performed using python (v3.8) and its libraries.⁴²

3 | RESULTS

3.1 | Glioblastoma

An example of axial dose distributions and DVH for a GBM patient case are shown in Figure 1. Dose metrics for all seven patient cases are summarized in Figure 2, in Table 3, and in Table S1. PTV dose metrics of all plans are always within the following limits: $D_{2\%} < 107\%$, $D_{98\%} > 90\%$, and $V_{95\%} > 95\%$. The main critical OAR was the brain for most patient cases and the PTV were mostly distant to other critical OAR of the head including eyes, lenses, and cochlea. For a few cases, the brain stem, chiasm and optical nerves received higher doses, but $D_{2\%}$ was always less than 54 Gy. Evaluated VHEE configurations with 200 MeV and 3 to 16 beams resulted in plan dose metrics, which were either not significantly different or which were significantly improved compared to the clinical IMRT reference plans. Notably, this also includes the VHEE configuration using only 3 beams. VHEE plans created using 5×100 MeV beams, resulted in significantly increased mean doses D_{mean} for the body (on average by 1 Gy) and the brain

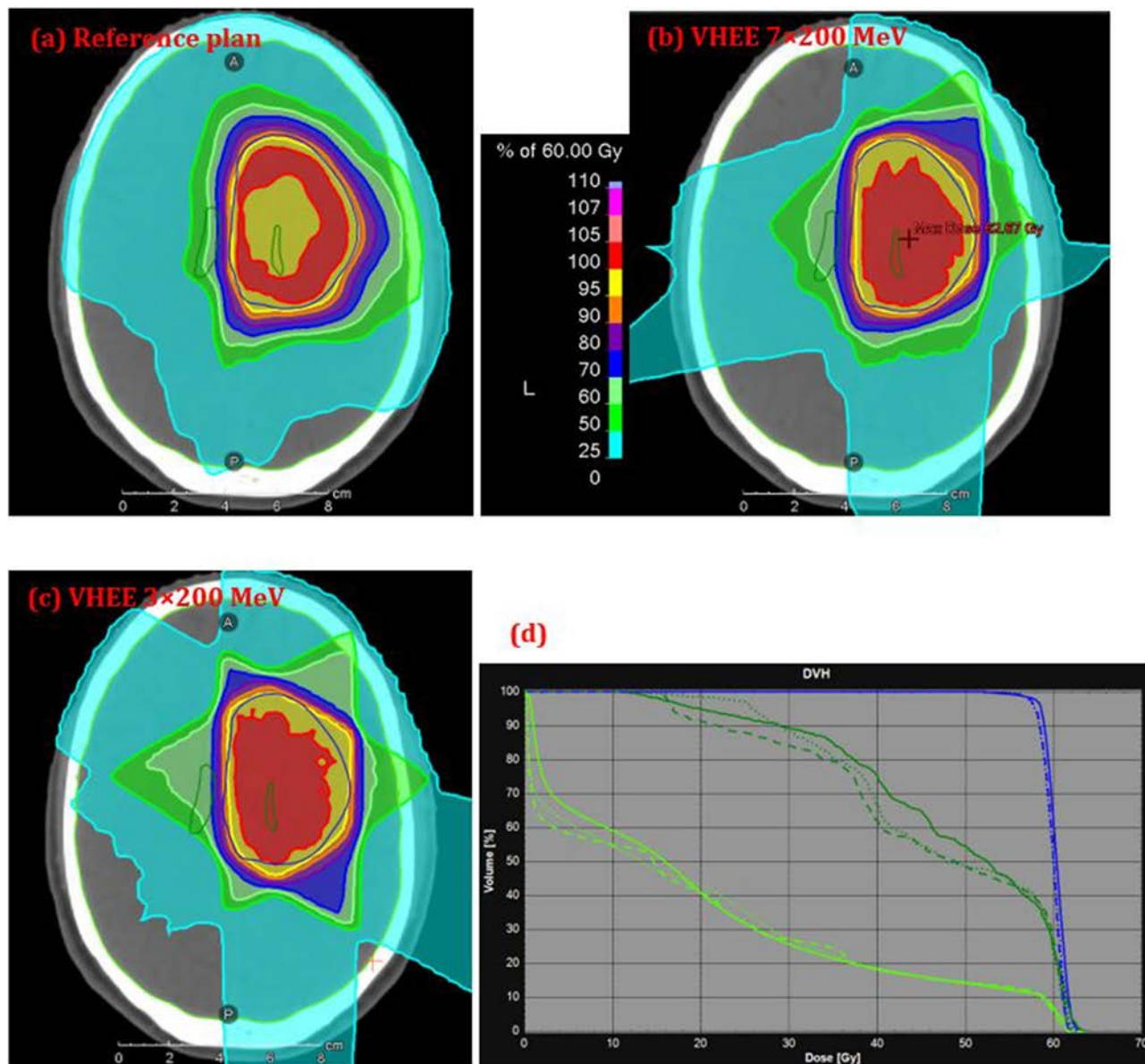


FIGURE 1 Treatment plan comparison for a glioblastoma case. Axial images of the clinical reference plan (a) (tomotherapy) and VHEE plans using the 7×200 MeV configuration (b) and the 3×200 MeV configuration (c). Panel (d) displays DVH for the planning target volume (dark blue), the ventricles (dark green), and the brain (light green) for the reference (solid lines), the 7×200 MeV (dotted lines), and the 3×200 MeV (dashed lines) plans. Doses to other critical OAR (chiasm, optical nerves, brain stem, spinal canal, cochlea, pituitary gland, lacrimal glands) are low ($D_{2\%} < 5$ Gy) and are therefore not displayed. DVH, dose-volume histograms; VHEE, very-high energy electron.

(on average by 2 Gy) and significantly increased near-maximum doses $D_{2\%}$ for the brain stem (on average by 6 Gy) and the chiasm (on average by 8 Gy). All other evaluated plan dose metrics for this configuration were either not significantly different or within 3% on average.

3.2 | Lung

Axial dose distributions and DVH for an exemplary lung cancer patient case are displayed in Figure 3. Dose

metrics for all seven patient cases are summarized in Figure 2, in Table 3, in Figure S1, and in Table S2. PTV dose metrics of all plans were always within the following limits: $D_{2\%} < 107\%$, $D_{98\%} > 90\%$, and $V_{95\%} > 93\%$. $V_{95\%}$ and $H_{98\%}$ of the PTV for VHEE plans did not significantly differ from the IMRT reference plans or were significantly improved for the VHEE plans. Two IMRT reference plans had a $V_{95\%}$ slightly below 95%. This was due to a slightly increased clinical emphasis on OAR sparing for these cases. D_{mean} of the body was found to be substantially increased for the 5×100 MeV and the 3×200 MeV configurations compared to the reference

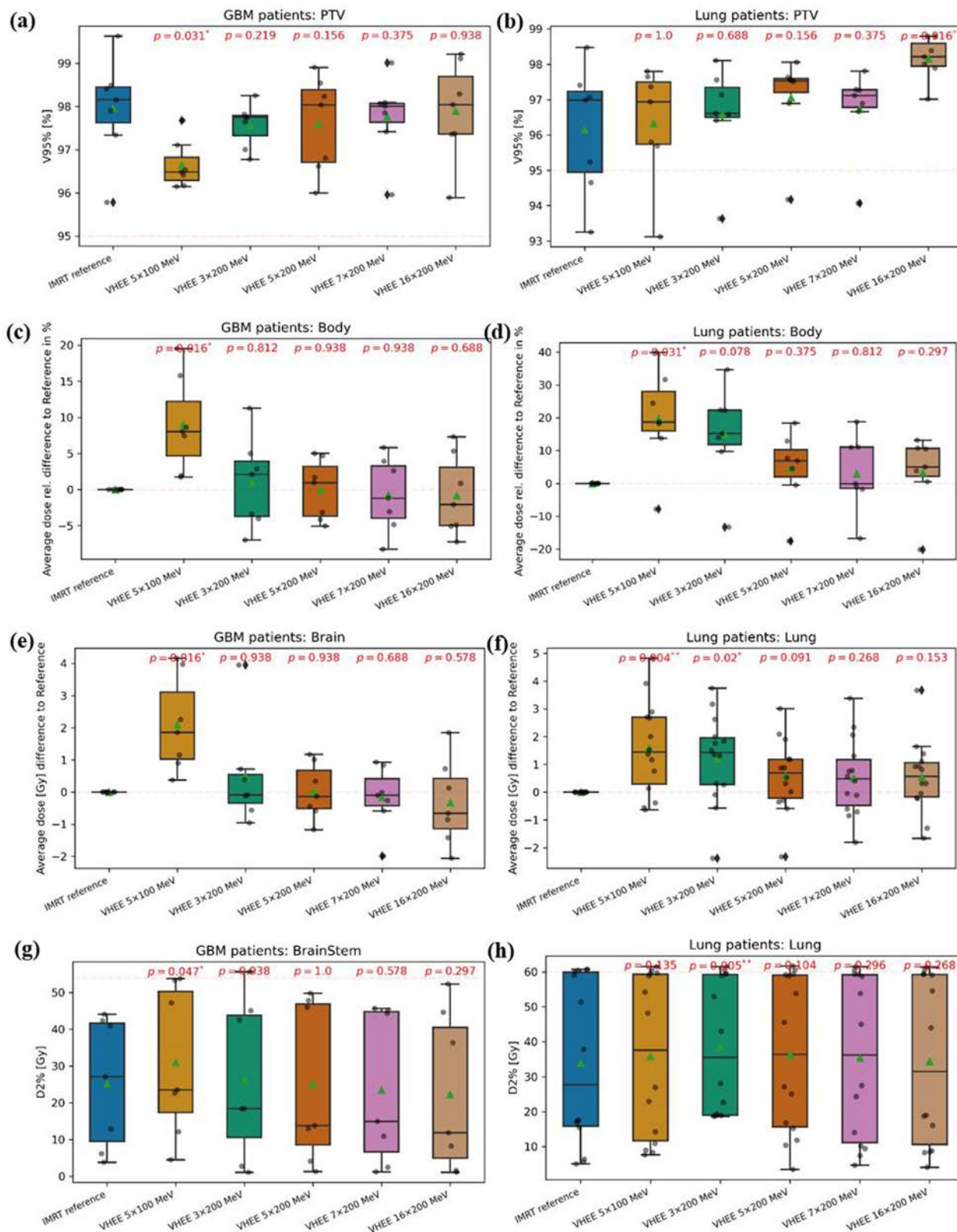


FIGURE 2 Box-and-whisker plots of PTV and OAR metrics for GBM patient cases (left panels) and lung cancer patient cases (right panels) planned with VHEE RT and compared to the clinical IMRT reference treatments. Values for individual structures are overlaid as scattered grey dots. Mean values are indicated by green triangles. p -values of the two-sided Wilcoxon signed-rank test of the VHEE planning technique with respect to the IMRT reference plan are provided in red above each VHEE column. Left and right lungs were pooled for combined evaluation. GBM, glioblastoma; IMRT, intensity-modulated photon radiation therapy; OAR, organ-at-risk; PTV, planning target volume; RT, radiation therapy; VHEE, very-high energy electron. Significance levels of $p < 0.05$, $p < 0.01$, $p < 0.001$ are indicated by *, **, and ***, respectively.

TABLE 3 Planning target volume and organs-at-risk dose metrics for the evaluated glioblastoma (a) and lung cancer (b) patient cases. Averages of dose metrics (over n structures) are provided for the intensity-modulated photon radiation therapy reference plans. For the VHEE plans, percentage differences of the dose metrics with respect to those of the reference plans are provided. Left-right symmetric organs were grouped for combined evaluation. Significant differences ($p < 0.05$) are highlighted in green (in favor of VHEE) and red (in favor of IMRT) if differences are larger than 3% and in yellow if differences are within 3% (in favor of one or the other).

(a)	Structure: n	PTV 7	Body 7	Brain 7	Brain stem 7	Chiasm 7	Optic nerve 14						
Planning technique	Dose metric:	$V_{95\%}$	$HI_{98\%}$	$D_{2\%}$	D_{mean}	$D_{2\%}$	D_{mean}	$D_{2\%}$	D_{mean}	$D_{2\%}$	D_{mean}	$D_{2\%}$	D_{mean}
IMRT reference	Mean value	98.0%	0.92	60.0 Gy	8.5 Gy	61.1 Gy	23.6 Gy	25.3 Gy	6.4 Gy	19.1 Gy	11.7 Gy	6.4 Gy	3.6 Gy
VHEE 5 × 100 MeV	Difference (%)	-1.3	-1.3	-0.6	9.9	0.3	8.9	22.5	1.2	43.3	12.5	6.7	9.5
VHEE 3 × 200 MeV	Difference (%)	-0.4	0.5	-0.3	1.9	-0.5	2.0	3.7	-32.1	-0.2	-30.6	27.8	13.3
VHEE 5 × 200 MeV	Difference (%)	-0.4	-0.7	-0.5	0.4	0.0	0.1	-0.8	-46.1	-15.5	-46.7	-40.8	-34.8
VHEE 7 × 200 MeV	Difference (%)	-0.2	0.3	-0.4	-0.3	-0.4	-0.7	-7.1	-50.3	-5.7	-46.0	-20.6	-28.1
VHEE 16 × 200 MeV	Difference (%)	-0.1	0.3	-0.4	0.0	-0.3	-1.4	-11.9	-52.5	-3.5	-42.9	-18.6	-27.2
(b)	Structure: n	PTV 7	Body 7	Lung 14	Esophagus 7	Trachea 7	Heart 7						
Planning technique	Dose metric:	$V_{95\%}$	$HI_{98\%}$	$D_{2\%}$	D_{mean}	$D_{2\%}$	D_{mean}	$D_{2\%}$	D_{mean}	$D_{2\%}$	D_{mean}	$D_{2\%}$	D_{mean}
IMRT reference	Mean value	96.2%	0.9	33.0 Gy	3.1 Gy	33.9 Gy	8.7 Gy	24.1 Gy	5.7 Gy	17.3 Gy	4.1 Gy	21.5	4.3
VHEE 5 × 100 MeV	Difference (%)	0.2	0.0	14.6	18.1	5.8	18.4	28.6	30.7	45.3	37.6	22.5	37.1
VHEE 3 × 200 MeV	Difference (%)	0.4	0.1	2.0	13.6	14.0	13.8	28.7	37.8	40.3	52.5	21.1	34.9
VHEE 5 × 200 MeV	Difference (%)	0.9	0.4	5.2	4.1	7.2	6.9	3.2	-0.4	19.2	-0.4	4.2	11.6
VHEE 7 × 200 MeV	Difference (%)	0.6	0.5	6.4	2.2	4.4	6.1	-3.8	-2.1	8.6	0.4	4.9	-5.6
VHEE 16 × 200 MeV	Difference (%)	2.1	1.7	0.1	2.5	1.4	6.3	2.0	-5.5	14.8	-0.6	1.3	13.2

Abbreviations: IMRT, intensity-modulated photon radiation therapy; OAR, organs-at-risk; PTV, planning target volume; VHEE, very-high energy electron.

plans, on average by 18% and 14%. Instead, for the other tested VHEE configurations with more beams, body D_{mean} were not significantly changed and on average within 5% of the reference plans. D_{mean} of the lung were significantly increased for the 3 × 200 MeV and the 5 × 100 MeV configurations, on average by about 1.5 Gy, whereas for the other configurations there were no significant differences and average differences were about 0.5 Gy. $V_{20\text{ Gy}}$ and $V_{5\text{ Gy}}$ of the lung were also significantly increased for the 3 × 200 MeV and the 5 × 100 MeV configurations. Instead, there were no significant differences for $V_{20\text{ Gy}}$ and $V_{5\text{ Gy}}$ for all other configurations. Similarly, $D_{2\%}$ and D_{mean} to the heart were increased by about 4 Gy and 1.5 Gy on average, respectively, for both 3 × 200 MeV and the 5 × 100 MeV configurations, whereas for the other VHEE configurations differences were not significant and on average within 1 Gy.

4 | DISCUSSION

Multiple initiatives set out to explore the clinical application of broad beam VHEE using UHDR^{21,27,31} and novel VHEE RT devices using a limited number of fixed beam portals are designed to deliver a whole treatment fraction on time scales compatible with those of pre-clinical irradiations that resulted in a substantial FLASH effect.²⁷ The achievable dosimetric plan quality is of concern when using only a few 3D-conformed broad VHEE beams and may therefore decisively influence patient selection for such a treatment modality. The objective of this work was therefore to evaluate if a VHEE machine with a few 3D conformal beams can provide competitive dose distributions (non-inferiority design) so that the FLASH effect would be on top of that instead of compensating for a lack of dosimetric

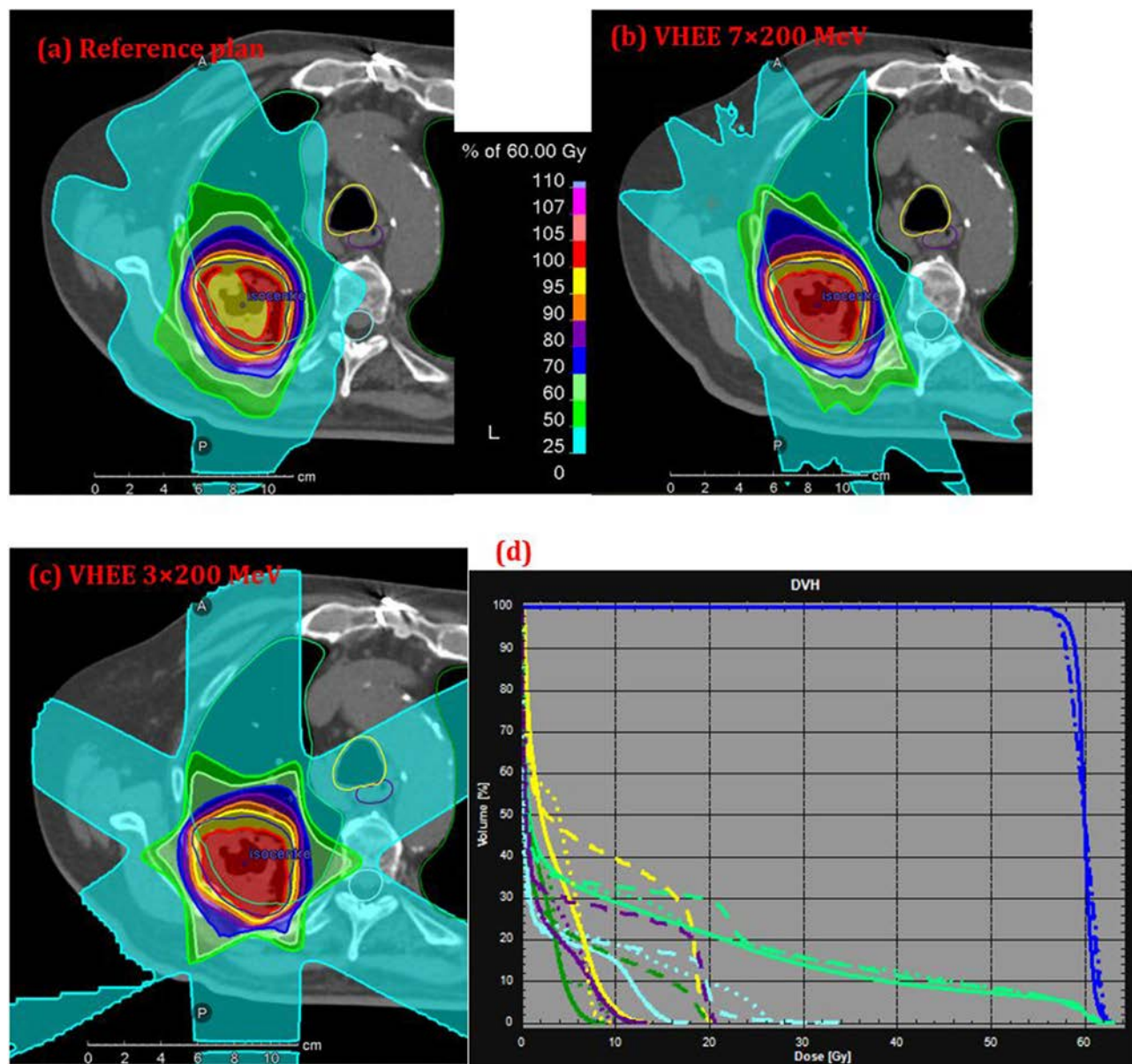


FIGURE 3 Treatment plan comparison for a lung cancer case. Axial images of the clinical reference plan (a) (Volumetric arc therapy) and VHEE plans using the 7×200 MeV configuration (b) and the 3×200 MeV configuration (c). Panel (d) displays DVH for the planning target volume (dark blue), lungs (dark and light green), trachea (yellow), esophagus (purple), and spinal canal (light blue) for the reference (solid lines), the 7×200 MeV (dotted lines), and the 3×200 MeV (dashed lines) plans. DVH, dose-volume histograms; VHEE, very-high energy electron.

conformity. This study demonstrates that such VHEE treatment approaches may provide conformal absorbed dose distributions with steep dose fall-offs already with a few (3 to 7) 3D-conformed broad VHEE beams for GBM and lung cancer patients. Furthermore, we found that the respective dose distributions are competitive with those obtained by standard-of-care photon IMRT techniques in terms of target coverage, homogeneity and OAR sparing. An increased biological selectivity due to normal tissue sparing by FLASH could therefore either contribute to improve the toxicity profile of GBM

and lung cancer treatments or make it possible to escalate doses delivered to the tumors.

Critical dose limiting toxicities (DLT) for GBM are found mostly in the high dose region inside and in close vicinity of the PTV. Critical OAR are the brain and may also include brain stem, optical nerves and chiasm for cases where the tumor is adjacent to those structures. For all tested configurations with 200 MeV, averaged $D_{2\%}$ and D_{mean} values of those OAR are either within 2 Gy and not significantly changed compared to the reference plans or a larger sparing is achieved by VHEE

on average, which is sometimes statistically significant. Instead, for the 5×100 MeV configuration there is an increase in the average D_{mean} for the brain of about 2 Gy. This dose increase can be mostly attributed to the larger lateral penumbra of lower energy VHEE beams and may be an incentive to select higher energy VHEE beams for treatments.²⁵ While configurations with more than 3 beams usually created more flexibility in OAR sparing, they generally only led to smaller improvements of dose metrics for the evaluated GBM cases. In contrast, configurations with 5 or more beams were found to improve dose metrics for lung cancer cases. VHEE configurations with 200 MeV and 5, 7 and 16 beams show non-significant but mostly slightly increased averaged D_{mean} for the lung and for the heart (at most about 0.6 Gy), compared to the reference plans. We found that the spinal canal, the esophagus, and the trachea were not OAR of principal clinical concern in terms of toxicity and they were consequently not considered a high priority for sparing during the optimization. Most important improvements of VHEE dose metrics were obtained for VHEE plans with 5 or more beams and with 200 MeV compared to plans with only 3 beams or 100 MeV. However, differences in dose metrics were patient-specific. For instance, Figure 1 displays a case, where using 7 instead of 3 beams did not result in important improvements of the DVH for both the PTV and the brain. Note that for configurations with 5 or more beams, the optimization process often resulted in some relative beams weights being low (<10%), so that the dose distribution was effectively determined by fewer beams (see for instance VHEE plans with 7 beams in Figure 1 and Figure 3). It is anticipated that better plans are achieved using only 5 or less VHEE beams if beam directions would also be optimized.⁴³

Our results suggest that 3D-conformal VHEE RT can be expected to provide a reasonable dosimetric conformity for simple, mostly convex target shapes with a limited number of critical OAR in close vicinity. Accordingly, one recent study suggested using two opposed collimated 40-MeV-electron beams for delivering pediatric whole brain UHDR RT.²¹ It is expected that for more complex clinical indications (e.g., target geometries with convex, partially disjunctive, large volumes and cases with multiple OAR in vicinity of the target), plan quality of 3D-conformal VHEE treatments could be substantially degraded compared to standard-of-care IMRT techniques, as this is generally observed when comparing 3D-CRT with IMRT techniques for photon beams.^{38,44,45} For such cases, intensity modulated (i.e., scanned) VHEE treatments may be more adequate and, indeed, several treatment planning studies have reported on intensity modulated VHEE techniques providing a dosimetrically superior plan quality compared to standard-of-care IMRT techniques, as previously mentioned.^{22–24,32–34} However, delivery of intensity modulated UHDR VHEE treatments

may prolong the time to deliver a field compared to 3D-conformal UHDR VHEE treatments and might therefore result in a reduction or disappearance of the FLASH effect.

Differences in OAR dose metrics between 3D-conformal VHEE RT and clinical IMRT reference plans obtained in this study are mostly below 10% (Table 3). This is small compared to the sparing that has been reported by some preclinical FLASH studies for brain and lung tissues with a DMF of 1.4 and more.³ Since the FLASH effect is expected to be the most pronounced in the high dose region,⁵ it may provide additional substantial and biologically-selective sparing of healthy tissues inside and in the vicinity of the PTV, if sufficient geometric sparing using steep dose gradients cannot be reached. This is particularly of interest for healthy tissues inside the GTV-to-PTV margin, which often encompasses a substantial fraction of the overall PTV volume. 3D-conformal UHDR VHEE treatments may therefore be clinically superior specifically for cases where DLT are encountered in the high dose region. While this work assesses only the absorbed dose distributions achieved by VHEE-based UHDR RT, future work is envisaged to encompass a quantitative assessment of the FLASH effect.

There are several limitations to the current work. The beam model we used assumes a homogenous parallel beam fluence at the isocenter, which is perfectly collimated without scattering in air. Instead, clinical electron machines of 4–25 MeV present with inhomogeneities in transverse fluence and dose profiles (~5%).^{46,47} Such inhomogeneous fluences may also be expected for future clinical VHEE RT devices that deliver broad beams. Furthermore, air, collimation devices, and other beam-interfering treatment head elements will produce scattered electrons and bremsstrahlung that will result in additional doses to the patient and may increase the lateral penumbra. The simulation of a more realistic beam phase space may further increase the lateral penumbra. Compared to the VHEE dose distributions presented here, all these factors may somewhat decrease dose homogeneity in the target and the dosimetric conformity. However, for larger depths, the penumbra of the VHEE beams is mostly driven by Coulomb scattering in the patient.^{25,41} Moreover, bremsstrahlung is mostly forward directed, and corresponding dose contributions may be factored in for treatment planning.⁴¹ To summarize, one can assume that the simulation of an idealized VHEE beam used in this study will only have a limited impact on our findings compared to simulations using a more realistic description of the VHEE beam and treatment head.

The 3D-conformal VHEE plans created for this work were optimized using forward planning (i.e., an iterative manual procedure to optimize dose distributions) and higher quality 3D-conformal VHEE plans would have been likely achieved if an inverse optimization approach

would have been used. A Collapsed Cone dose engine was used to compute clinical plans for MV photons. Instead, a Monte Carlo dose engine was used to obtain dose distributions for VHEE plans. Monte Carlo dose computations are generally regarded to be the gold standard for treatment planning in RT and are known to result in more accurate but also in more unfavorable dose distributions compared to simpler dose computation techniques, especially in heterogeneous anatomies such as lungs.⁴⁶ This may somewhat bias comparisons between IMRT reference plans and the VHEE plans presented here. On the other hand, dose distributions of VHEE beams were reported to be less perturbed by heterogeneities compared to photon beams and more robust to anatomical changes compared to proton beams.^{48,49} This increased dosimetric robustness may be a further asset for VHEE RT.

5 | CONCLUSIONS

This study shows that simple target shapes in the brain and thorax may be conformally treated using 3D-conformal VHEE RT delivery with a number of beams as low as 3 to 7 without the use of intensity modulation and that a dosimetric plan quality comparable to standard-of-care intensity-modulated photon RT can be achieved. UHDR FLASH treatments using such 3D-conformal VHEE delivery may facilitate shorter overall delivery times (~100 ms) compared with intensity-modulated and pencil beam scanning delivery techniques, thereby potentially optimizing the FLASH effect. Hence, quasi-simultaneously delivered 3D-conformal UHDR VHEE beams represent a promising option for the initial clinical exploration of the FLASH effect using external beam UHDR RT for deep-seated tumors.

ACKNOWLEDGEMENTS

This research has been funded by the ISREC Foundation thanks to a Biltrema donation, and partially funded by the Fondation pour le soutien de la recherche et du développement de l'oncologie (FSRDO).

Open access funding provided by Universite de Lausanne.

CONFLICTS OF INTEREST STATEMENT

E. Traneus is an employee of RaySearch Laboratories AB.

DATA AVAILABILITY STATEMENT

The data that support the findings of this study are available from the corresponding author upon reasonable request.

ORCID

Till Tobias Böhlen 

<https://orcid.org/0000-0001-7408-0187>

Raphaël Moeckli 

<https://orcid.org/0000-0002-5885-934X>

REFERENCES

- Favaudon V, Caplier L, Monceau V, et al. Ultrahigh dose-rate FLASH irradiation increases the differential response between normal and tumor tissue in mice. *Sci Transl Med*. 2014;6(245):245ra93.
- Vozenin MC, Bourhis J, Durante M. Towards clinical translation of FLASH radiotherapy. *Nat Rev Clin Oncol*. 2022 ;19(12):791-803. Accessed October 31, 2022. <https://www.nature.com/articles/s41571-022-00697-z>. [Internet].
- Vozenin MC, Hendry JH, Limoli CL. Biological benefits of ultrahigh dose rate FLASH radiotherapy: sleeping beauty awoken. *Clin Oncol*. 2019;31(7):407-415. doi:10.1016/j.clon.2019.04.001. [Internet].
- Böhlen TT, Germond JF, Petersson K, et al. Effect of conventional and ultra-high dose rate "FLASH" irradiations on preclinical tumour models: a systematic analysis. *Int J Radiat Oncol Biol Phys*. doi:10.1016/j.ijrobp.2023.05.045. [Internet]. 2023 [cited 2023 Jun 6];S0360301623005357. Available from: <https://linkinghub.elsevier.com/retrieve/pii/S0360301623005357>
- Böhlen TT, Germond JF, Bourhis J, et al. Normal tissue sparing by FLASH as a function of single-fraction dose: a quantitative analysis. *Int J Radiat Oncol Biol Phys*. 2022;114(5):1032-1044. Accessed November 15, 2022. <https://linkinghub.elsevier.com/retrieve/pii/S0360301622005417>. [Internet].
- Bourhis J, Sozzi WJ, Gonçalves Jorge P, et al. Treatment of a first patient with FLASH-radiotherapy. *Radiother Oncol*. 2019;139:18-22. Accessed March 4, 2021. <https://linkinghub.elsevier.com/retrieve/pii/S0167814019329597>. [Internet].
- Gaide O, Herrera F, Sozzi WJ, et al. Comparison of ultrahigh versus conventional dose rate radiotherapy in a patient with cutaneous lymphoma. *Radiother Oncol*. 2022;174:87-91. Accessed January 21, 2022. <https://linkinghub.elsevier.com/retrieve/pii/S0167814021090939>. [Internet].
- Bourhis J, FLASH Radiotherapy for Skin Cancer (LANCE).[Internet]. National Library of Medicine; 2023 Accessed May 14, 2022. <https://clinicaltrials.gov/ct2/show/NCT05724875>
- Mascia AE, Daugherty EC, Zhang Y, et al. Proton FLASH radiotherapy for the treatment of symptomatic bone metastases: the FAST-01 nonrandomized trial. *JAMA Oncol*. 2023;9(1):62-69. Accessed October 26, 2022. <https://jamanetwork.com/journals/jamaoncology/fullarticle/2797843>. [Internet].
- Breneman J. FLASH radiotherapy for the treatment of symptomatic bone metastases in the thorax (FAST-02) NCT05524064 [Internet]. National Library of Medicine; 2022 Accessed December 23, 2022. <https://clinicaltrials.gov/ct2/show/NCT05524064?term=FLASH+FAST02&draw=2&rank=1>
- Lyu Q, Neph R, O'Connor D, Ruan D, Boucher S, Sheng K. ROAD: rOtational direct Aperture optimization with a decoupled ring-collimator for FLASH radiotherapy. *Phys Med Biol*. 2021;66(3):035020. Accessed August 2, 2021. <https://iopscience.iop.org/article/10.1088/1361-6560/abcdb0>. [Internet].
- Verhaegen F, Wanders RG, Wolfs C, Eekers D. Considerations for shoot-through FLASH proton therapy. *Phys Med Biol*. 2021;66(6):06NT01. Accessed January 15, 2022. <https://iopscience.iop.org/article/10.1088/1361-6560/abe55a>. [Internet].
- van de Water S, Safai S, Schippers JM, Weber DC, Lomax AJ. Towards FLASH proton therapy: the impact of treatment planning and machine characteristics on achievable dose rates. *Acta Oncol (Madr)*. 2019;58(10):1463-1469. doi:10.1080/0284186X.2019.1627416. [Internet].
- Folkerts MM, Abel E, Busold S, Perez JR, Krishnamurthi V, Ling CC. A framework for defining FLASH dose rate for pencil beam scanning. *Medical Physics*. 2020;47(12):6396-6404.

- Accessed April 26, 2021. <https://onlinelibrary.wiley.com/doi/10.1002/mp.14456>. [Internet].
15. Zhang G, Wang J, Wang Y, Peng H. Proton FLASH: passive scattering or pencil beam scanning? *Phys Med Biol*. 2021;66(3):03NT01. Accessed August 24, 2021. <https://iopscience.iop.org/article/10.1088/1361-6560/abd22d>. [Internet].
 16. Jolly S, Owen H, Schippers M, Welsch C. Technical challenges for FLASH proton therapy. *Phys Medica*. 2020;78:71-82. Accessed February 9, 2021. <https://linkinghub.elsevier.com/retrieve/pii/S1120179720301964>. [Internet].
 17. Weber UA, Scifoni E, Durante M. FLASH radiotherapy with carbon ion beams. *Medical Physics*. 2022;49(3):1974-1992. Accessed March 25, 2022. <https://onlinelibrary.wiley.com/doi/10.1002/mp.15135>. [Internet].
 18. Simeonov Y, Weber U, Schuy C, et al. Monte Carlo simulations and dose measurements of 2D range-modulators for scanned particle therapy. *Zeitschrift für Medizinische Physik*. 2021;31(2):203-214. Accessed July 13, 2021. <https://linkinghub.elsevier.com/retrieve/pii/S0939388920300672>. [Internet].
 19. Simeonov Y, Weber U, Penchev P, et al. 3D range-modulator for scanned particle therapy: development, Monte Carlo simulations and experimental evaluation. *Phys Med Biol*. 2017;62(17):7075-7096. Accessed January 19, 2021. <https://iopscience.iop.org/article/10.1088/1361-6560/aa81f4>. [Internet].
 20. Maxim PG, Tantawi SG, Loo BW. PHASER: a platform for clinical translation of FLASH cancer radiotherapy. *Radiother Oncol*. 2019;139:28-33. doi:10.1016/j.radonc.2019.05.005. [Internet].
 21. Breikreutz DY, Shumail M, Bush KK, Tantawi SG, Maxime PG, Loo BW. Initial steps towards a clinical FLASH radiotherapy system: pediatric whole brain irradiation with 40 MeV electrons at FLASH dose rates. *Radiat Res*. 2020;194(6):594-599.
 22. Schüler E, Eriksson K, Hynning E, et al. Very high-energy electron (VHEE) beams in radiation therapy; Treatment plan comparison between VHEE, VMAT, and PPBS. *Med Phys*. 2017;44(6):2544-2555.
 23. Palma B, Bazalova-Carter M, Hårdemark B, et al. Assessment of the quality of very high-energy electron radiotherapy planning. *Radiother Oncol*. 2016;119(1):154-158. Accessed March 3, 2021. <https://linkinghub.elsevier.com/retrieve/pii/S0167814016000487>. [Internet].
 24. Bazalova-Carter M, Qu B, Palma B, et al. Treatment planning for radiotherapy with very high-energy electron beams and comparison of VHEE and VMAT plans. *Med Phys*. 2015;42(5):2615-2625. Accessed March 3, 2021. <http://doi.wiley.com/10.1118/1.4918923>. [Internet].
 25. Böhlen TT, Germond J, Traneus E, et al. Characteristics of very high-energy electron beams for the irradiation of deep-seated targets. *Medical Physics*. 2021;48(7):3958-3967. Accessed January 4, 2023. <https://onlinelibrary.wiley.com/doi/10.1002/mp.14891>. [Internet].
 26. Ronga MG, Cavallone M, Patriarca A, et al. Back to the future: very high-energy electrons (VHEEs) and their potential application in radiation therapy. *Cancers*. 2021;13(19):4942. Accessed October 15, 2021. <https://www.mdpi.com/2072-6694/13/19/4942>. [Internet].
 27. CHUV press release. CHUV, CERN and THERYQ join forces for a world first in cancer radiotherapy. CHUV press release; 2022. [Internet] Accessed December 21, 2022. <https://www.chuv.ch/fr/chuv-home/espace-pro/journalistes/communiqués-de-presse/detail/chuv-cern-and-theryq-join-forces-for-a-world-first-in-cancer-radiotherapy>
 28. Friedl AA, Prise KM, Butterworth KT, Montay-Gruel P, Favaudon V. Radiobiology of the FLASH effect. *Med Phys*. 2022;49(3):1993-2013. Accessed September 28, 2021. <https://onlinelibrary.wiley.com/doi/10.1002/mp.15184>. [Internet].
 29. Rahman M, Trigilio A, Franciosini G, Moeckli R, Zhang R, Böhlen TT. FLASH radiotherapy treatment planning and models for electron beams. *Radiat Oncol*. 2022;175:210-221. Accessed March 16, 2023. <https://linkinghub.elsevier.com/retrieve/pii/S016781402204230X>. [Internet].
 30. Böhlen TT, Germond JF, Bochud F, et al. In reply to Horst et al. *Int J Radiat Oncol Biol Phys*. 2023;115(4):1007-1009. <https://www.sciencedirect.com/science/article/pii/S0360301622035301>. [Internet].
 31. Faillace L, Alesini D, Bisogni G, et al. Perspectives in linear accelerator for FLASH VHEE: study of a compact C-band system. *Physica Medica*. 2022;104:149-159. Accessed December 5, 2022. <https://linkinghub.elsevier.com/retrieve/pii/S1120179722020798>. [Internet].
 32. Yeboah C, Sandison GA. Optimized treatment planning for prostate cancer comparing IMPT, VHEET and 15 MV IMXT. *Phys Med Biol*. 2002;47(13):2247-2261. Accessed September 15, 2020. <https://iopscience.iop.org/article/10.1088/0031-9155/47/13/305>. [Internet].
 33. Yeboah C, Sandison GA, Moskvina V. Optimization of intensity-modulated very high energy (50–250 MeV) electron therapy. *Phys Med Biol*. 2002;47(8):1285-1301. Accessed March 3, 2021. <https://iopscience.iop.org/article/10.1088/0031-9155/47/8/305>. [Internet].
 34. Fuchs T, Szymanowski H, Oelfke U, et al. Treatment planning for laser-accelerated very-high energy electrons. *Phys Med Biol*. 2009;54(11):3315-3328.
 35. Wen PY, Weller M, Lee EQ, et al. Glioblastoma in adults: a Society for Neuro-Oncology (SNO) and European Society of Neuro-Oncology (EANO) consensus review on current management and future directions. *Neuro-Oncology*. 2020;22(8):1073-1113. Accessed October 17, 2022. <https://academic.oup.com/neuro-oncology/article/22/8/1073/5824407>. [Internet].
 36. Remon J, Soria JC, Peters S. Early and locally advanced non-small-cell lung cancer: an update of the ESMO Clinical Practice Guidelines focusing on diagnosis, staging, systemic and local therapy. *Annals of Oncology*. 2021;32(12):1637-1642. Accessed February 27, 2023. <https://linkinghub.elsevier.com/retrieve/pii/S0923753421042794>. [Internet].
 37. Bourhis J, Montay-Gruel P, Gonçalves Jorge P, et al. Clinical translation of FLASH radiotherapy: why and how? *Radiother Oncol*. 2019;139:11-17. Accessed March 4, 2021. <https://linkinghub.elsevier.com/retrieve/pii/S0167814019303603>. [Internet].
 38. Amelio D, Lorentini S, Schwarz M, Amichetti M. Intensity-modulated radiation therapy in newly diagnosed glioblastoma: a systematic review on clinical and technical issues. *Radiotherapy and Oncology*. 2010;97(3):361-369. Accessed September 16, 2021. <https://linkinghub.elsevier.com/retrieve/pii/S0167814010005232>. [Internet].
 39. Kling A, Barão F, Nakagawa M, Távoraand L, Vaz P. Advanced Monte Carlo for Radiation Physics, Particle Transport Simulation and Applications - Proceedings of the Monte Carlo 2000 Conference. 23–26 October 2000. Springer; 2014.
 40. Kawrakow I, Fippel M. VMC++, a fast MC algorithm for radiation treatment planning. In: Schlegel W, Bortfeld T, eds. *The use of Computers in Radiation Therapy*. Springer; 2000:126-128. Accessed March 4, 2021. http://link.springer.com/10.1007/978-3-642-59758-9_46. [Internet].
 41. DesRosiers C, Moskvina V, Bielajew AF, Papiez L. 150–250 MeV electron beams in radiation therapy. *Phys Med Biol*. 2000;45(7):1781-1805.
 42. Van Rossum G, Drake FL. *The Python Language Reference*. Python Software Foundation; 2010. Release 3.0.1.
 43. Schipaanboord BWK, Heijmen BJM, Breedveld S. TBS-BAO: fully automated beam angle optimization for IMRT guided by a total-beam-space reference plan. *Phys Med Biol*. 2022;67(3):035004. Accessed February 7, 2023. <https://iopscience.iop.org/article/10.1088/1361-6560/ac4b37>. [Internet].

44. Lorentini S, Amelio D, Giri MG, et al. IMRT or 3D-CRT in Glioblastoma? A dosimetric criterion for patient selection. *Technol Cancer Res Treat*. 2013;12(5):411-420. Accessed September 16, 2021. <http://journals.sagepub.com/doi/10.7785/tcrt.2012.500341>. [Internet].
45. Grills IS, Yan D, Martinez AA, Vicini FA, Wong JW, Kestin LL. Potential for reduced toxicity and dose escalation in the treatment of inoperable non-small-cell lung cancer: a comparison of intensity-modulated radiation therapy (IMRT), 3D conformal radiation, and elective nodal irradiation. *Int J Radiat Oncol Biol Phys*. 2003;57(3):875-890. Accessed September 16, 2021. <https://linkinghub.elsevier.com/retrieve/pii/S0360301603007430>. [Internet].
46. Chetty IJ, Curran B, Cygler JE, et al. Report of the AAPM Task Group No. 105: issues associated with clinical implementation of Monte Carlo-based photon and electron external beam treatment planning. *Med Phys*. 2007;34(12):4818-4853. http://www.ncbi.nlm.nih.gov/entrez/query.fcgi?cmd=Retrieve&db=PubMed&dopt=Citation&list_uids=18196810
47. Smilowitz JB, Das IJ, Feygelman V, et al. AAPM Medical Physics Practice Guideline 5.a.: commissioning and QA of treatment planning dose calculations - megavoltage photon and electron beams. *J Appl Clin Med Phys*. 2015;16(5):14-34. Accessed March 17, 2021. <http://doi.wiley.com/10.1120/jacmp.v16i5.5768>. [Internet].
48. Lagzda A, Angal-Kalinin D, Jones J, et al. Influence of heterogeneous media on Very High Energy Electron (VHEE) dose penetration and a Monte Carlo-based comparison with existing radiotherapy modalities. *Nucl Instrum Methods Phys Res, B*. 2020;482:70-81. Accessed October 6, 2020. <https://linkinghub.elsevier.com/retrieve/pii/S0168583220304043>. [Internet].
49. Lagzda A, Jones RM, Angal-Kalinin D, et al. Relative insensitivity to inhomogeneities on very high energy electron dose distributions. In: Proceedings of IPAC2017. 2017:4791-4794.

SUPPORTING INFORMATION

Additional supporting information can be found online in the Supporting Information section at the end of this article.

How to cite this article: Böhlen TT, Germond JF, Traneus E, et al. 3D-conformal very-high energy electron therapy as candidate modality for FLASH-RT: A treatment planning study for glioblastoma and lung cancer. *Med Phys*. 2023;50:5745–5756.
<https://doi.org/10.1002/mp.16586>